

## Earthquake observation of deeply embedded building structure

M. Watakabe

*Institute of Construction Technology, Toda Corporation, Tokyo, Japan*

H. Matsumoto, K. Ariizumi, Y. Fukahori & Y. Shikama

*Engineering Research Center, Tokyo Electric Power Company, Japan*

K. Yamanouchi & H. Kuniyoshi

*Architecture & Structural Technical Department, Tokyo Electric Power Services Co., Ltd, Japan*

**ABSTRACT:** Earthquake observation of the deeply embedded building structure in the suburbs of Tokyo has been continued on a large scale for the purpose of investigation of dynamic soil-structure interaction behavior. Many earthquake records have been obtained since June, 1985. The amplitude in the structure decreases to about half of that of the soil in a frequency range higher than the first natural frequency of the structure, and is in accordance to the frequencies. By comparison between the normalized spectra of the dynamic lateral pressure and those of the velocities at approximately the same depth, the both shapes of the spectra closely coincide. Dynamic lateral pressures obtained by the response analysis of two dimensional finite element method(FEM) are coincident to these of observation results.

### 1 INTRODUCTION

Earthquake observation has been carried out at many building structures to investigate the dynamic soil-structure interaction behavior in Japan(See Tsubokura et al. 1983, etc). Up till now, however, there has been little research related to the behavior of dynamic lateral pressures acting on the basement walls of deeply embedded building structures. In this paper, the authors wish to introduce the investigation of the fundamental characteristics of earthquake records observed in and around deeply embedded building structures and of the dynamic lateral pressure acting on the basement walls during earthquakes. The response analyses by two-dimensional FEM was carried out to estimate fundamental characteristics of the soil-structure interaction behavior of the embedded building structure based on several earthquakes.

### 2 OUTLINE OF EARTHQUAKE OBSERVATION SYSTEM

#### 2.1 Outline of the ground, the building and observation system

Earthquake observation of the deeply embedded building structure has been continued on a large scale in the suburbs of Tokyo(See Fig.1). Ground conditions around the building and cross-section of building are as summarized in Fig. 2(a),(b), respectively. Geological structure consists of soft alluvial deposits above thirty two meters and underlying diluvial deposits. About forty two meters below the ground surface,

there exists a firm diluvial deposit, generally called the "Upper Tokyo Formation", which is selected as the bearing stratum of the building.

Earthquakes were observed with arrays set up inside the building and those set up vertically in the ground about one meter and about 12 meters from the building, respectively. Seismometers were installed in the building (4 sets, 12 components), in the ground about one meter from the basement wall (panel A) (3 sets, 9 components), and in the ground about 12 meters from the basement wall (panel D) (4 sets, 12 components) as shown in Fig. 2(b). Dynamic earth and water pressures were observed during earthquake observation using 20 gauges (20 components) installed on the basement walls (See Fig. 2(b)).

#### 2.2 Observed earthquakes

As of March 1990, many earthquakes have been observed since June 1985 when earthquake observation began. The locations of the epicenters of these earthquake are as shown in Fig. 3. For the purposes of this study, 21 earthquakes (See Sakai et al. 1989) were chosen under condition of 2 or more intensity in Tokyo(Japanese Meteorological Agency Scale) and a maximum peak acceleration value of  $3\text{cm/sec}^2$  or more observed at GL-142m.

### 3 ANALYSIS OF OBSERVED RECORDS

#### 3.1 Maximum velocity distribution

On the basis of observed records, the ratios

of the maximum velocity at each observation point in the soil and in the building to the maximum velocity at GL-142m were determined. The mean values and standard deviations of the ratios obtained are as shown in Fig. 4. Both the horizontal and vertical components of velocity at GL-25.9m in the ground about 12 meters from the building were amplified by as low as 1.5 times on average. By contrast, they were more amplified above this level. Also, near the ground surface, the horizontal component was amplified by about 2.3 times on average and the vertical component by about 3.7 times on average. In the building, although amplification was observed at PH2, the horizontal component at B6F and 1F was amplified by as low as about 1.3 times and 1.5 times on average, respectively, indicating the effects on the embedment of the building.

### 3.2 Amplitude characteristics of the soil and the building

Correlation analysis was conducted on combinations of observed values obtained at two points in Array 1 as shown in Fig. 5, which was vertically set in the soil. The mean spectral ratios and standard deviations of GL-42m/GL-142m and GL-1.5m/GL-142m (horizontal component) were obtained as shown in Fig. 6(a) and (b), respectively, which represent transfer characteristics. Fourier spectra on smoothed by Parzen window having a bandwidth of 0.2 Hz are employed in this analysis. Fig. 6(a) shows that the primary frequency was predominant at around 0.71 Hz, while no predominance was observed in the secondary or higher mode of oscillation. In Fig. 6(b), predominance was observed at frequencies 0.71 Hz, 1.6 Hz, 2.56 Hz and 3.2 Hz, which indicated that predominant frequencies in higher modes of oscillation having a frequency of 1.60Hz or above were produced in shallow layers at GL-42m or above.

In order to investigate transfer characteristics between the ground and the building, the spectral ratio at each level was calculated using data observed in the ground at levels roughly corresponding to those observed at B6F and 1F. The results of this calculation are as shown in Fig. 7 (a) and (b), respectively. From the comparison between the spectrum at basement (B6F) and that in the soil layer at the depth of 25.9m, it is found that in the frequency range higher than the first natural frequency of the structure, the amplitude in the structure decreases to about half of that in the soil, and is accordance to the frequencies. The spectral ratio of 1F to GL-1.5m showed a similar tendency as estimated above. These phenomena indicated that dynamic soil-structure interaction occurred.

## 4 FUNDAMENTAL CHARACTERISTICS OF DYNAMIC LATERAL PRESSURE ON BASEMENT WALLS

### 4.1 Distribution of maximum dynamic lateral pressure

The mean values and standard deviations of the maximum dynamic lateral pressures on the basement walls are as shown in Fig. 8, in which the dynamic lateral pressure herein described signifies the fluctuation of earth pressure due to earthquake. The maximum dynamic lateral pressures shown in Fig. 8 are normalized by the maximum velocities at GL-142m. Fig. 9 shows variation coefficients between the maximum dynamic lateral pressures normalized by the maximum velocities and by the maximum accelerations at GL-142m, respectively. The variation coefficients of the maximum dynamic lateral pressures normalized by the maximum velocities are lower than those normalized by the maximum accelerations, and the variations in the vertical direction, smaller.

### 4.2 Frequency characteristics of dynamic lateral pressure

Fourier spectra was normalized by the maximum values. These spectra consist of dynamic lateral pressures acting on panels A and D at the ground surface level and the foundation level, and of observed velocities at the corresponding levels of the soil. Their mean values and standard deviations are as shown in Fig. 10(a), (b) and (c), respectively. Spectra determined from observed dynamic lateral pressures showed good agreement with spectra of velocities observed at almost the same levels. This result indicates that observed dynamic lateral pressures and velocities were interrelated, though qualitatively.

## 5 RESPONSE ANALYSIS

### 5.1 Analytical Model

Dynamic response analyses to estimate soil-structure interaction were carried out using the computer program "Super FLUSH" (See Kozou Keikaku Engineering, INC. 1988). The model employed in the analyses is as shown in Fig. 11. The soil was modeled to the plane strain element, the building to the lumped mass stick model and the basement wall to the solid element.

A semi-infinite half space was assumed at the bottom of the FEM model and the energy transmitting boundaries were attached at the both sides of FEM model to simulate the existence of semi-infinite soil layers. The shear wave velocities used in the analyses were estimated by the identified technique

(See Matsumoto et al. 1991). The damping ratios used in the analyses are assumed to the constant of 3% for soil layers and 5% for all structural components.

The input earthquake ground motion at the bottom of the FEM model was evaluated by the one dimensional wave propagation theory. The earthquake ground motion recorded at the depth of 142m was used as the control motion to estimate the input motion. Five earthquake ground motions evaluated above are used in the response analysis.

## 5.2 Response Analysis

The examples of the comparison between the computed waveforms and recorded ones are shown in Fig.12 and of the response spectra in Fig. 13, respectively.

The mean values and standard deviations of the observed maximum velocity are compared with the computed ones as shown in Fig. 14. The maximum values were normalized by the maximum velocities at the depth of 142m. Although the maximum values obtained by response analyses were rather smaller than observed ones on average, the distributions of maximum velocities were the similar tendency.

The mean values and standard deviations of the observed maximum dynamic lateral pressures on the basement walls and the computed ones are as shown in Fig.15. The maximum dynamic lateral pressures were normalized by the maximum velocities at the depth of 142m. The distribution of dynamic lateral pressures obtained by dynamic response analyses showed good agreement to the observed ones, except the near surface. The mean values and standard deviations of the velocity response spectrum ratio at the GL-1.5m and 1F are as shown in Fig. 16. The observed average value of the ground surface showed good agreement with the analyzed ones. On the other hand, the response spectrum at first floor obtained by response analyses underestimated to the observed one.

## 6 CONCLUSIONS

Analysis on the fundamental characteristics of earthquake records observed in and around deeply embedded building structures was carried out, and as a next step, the effect of dynamic soil-structure interaction by analyzing a two-dimensional FEM interaction model is investigated. The following results have been obtained.

(1) The amplification factor of the ground against GL-142m was as low as 1.5 or so on average (both horizontal and vertical) at GL-25.9m, while that at the ground surface level was about 2.3 (horizontal) and 3.7 (vertical) on average. The amplification factor of the building at the 6th basement level was about 1.3 (horizontal) on average, and that at the

1st floor level, about 1.5 on average. These results indicate the effects on the embedment of the building.

(2) Spectrum ratios between the soil and the building at the levels of (1F/GL-1.5m) and (B6F/ GL-25.9m) were examined. From comparison between the spectrum at basement (B6F) and that in the soil layer at the depth of 25.9m, it is found that in a frequency range higher than the first natural frequency of the structure, the amplitude in the structure decreases to about half of that in the soil, and is in accordance to the frequencies. The spectral ratio of 1F to GL-1.5m showed a similar tendency as estimated above. These phenomena indicated that dynamic soil-structure interaction occurred.

(3) The maximum dynamic lateral pressure requires a smaller variation coefficient and a smaller vertical variation when normalized by the maximum velocity than by the maximum acceleration. Spectra determined from observed dynamic lateral pressures showed good agreement with spectra of velocities observed at almost the same levels. This result indicates that observed dynamic lateral pressures and velocities were interrelated, though qualitatively.

(4) Although the maximum values obtained by dynamic response analyses were rather smaller than observed ones on average, the model employed in the analyses was available to estimate the soil-structure interaction.

## REFERENCES

- Sakai, Y., et al. 1989. Earthquake Observation of Deeply Embedded Building (in Japanese). Annual Meeting of A.I.J., 267-268.
- Tsubokura, H., et al. 1983. Observation and Analysis of Earthquake Motions to Deeply Embedded Underground Structure (in Japanese). Annual Meeting of A.I.J., 779-780.
- Kozo Keikaku Engineering, INC. 1988. Super FLUSH Manual.
- Matsumoto, H., et al. 1991. Earthquake Observation of Deeply Embedded Building, Sixth Canadian Conference on Earthquake Engineering.

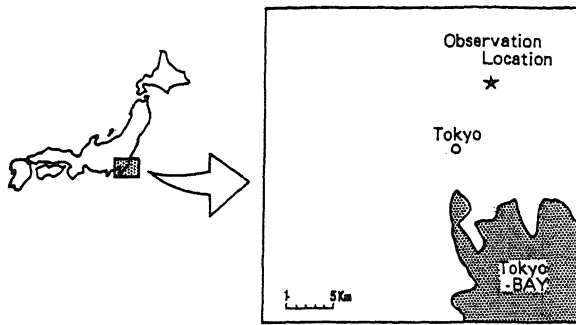
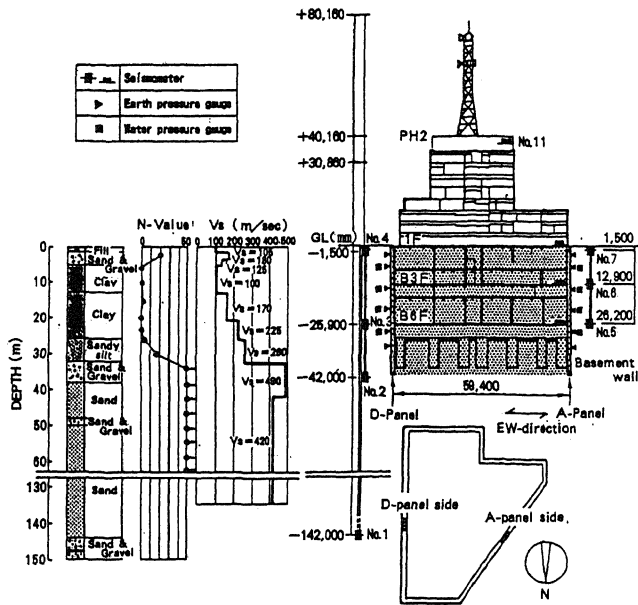


Fig.1 Observation location



(a) Soil profile (b) Location of observation points  
Fig.2 Outline of soil profile and building structure

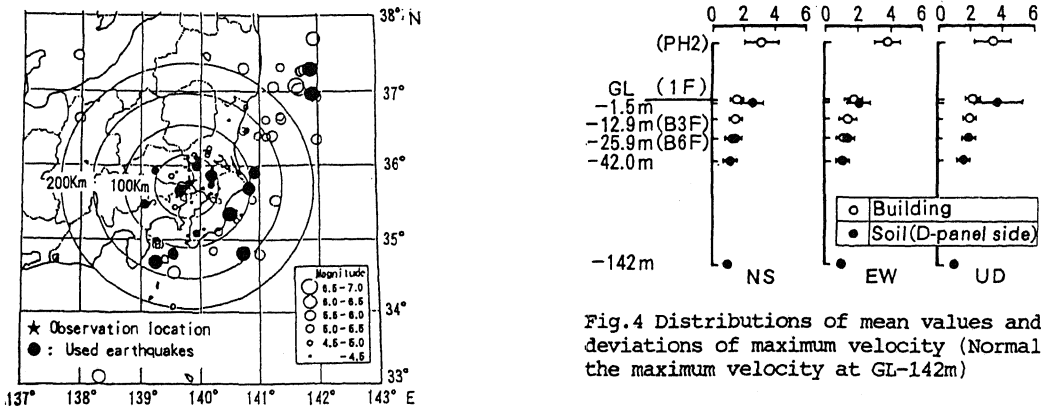


Fig.3 Location of epicenter and magnitude for observed earthquakes

Fig.4 Distributions of mean values and standard deviations of maximum velocity (Normalized by the maximum velocity at GL-142m)

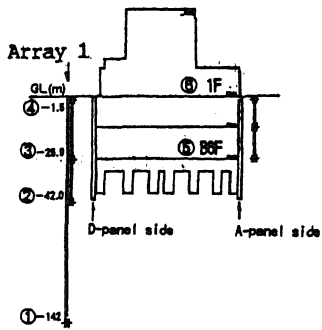


Fig.5 Arrangement of observation points

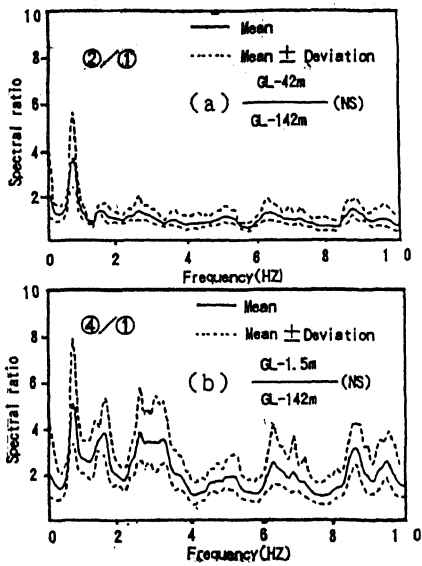


Fig.6 Averaged spectral ratio of soil layer (NS-direction)

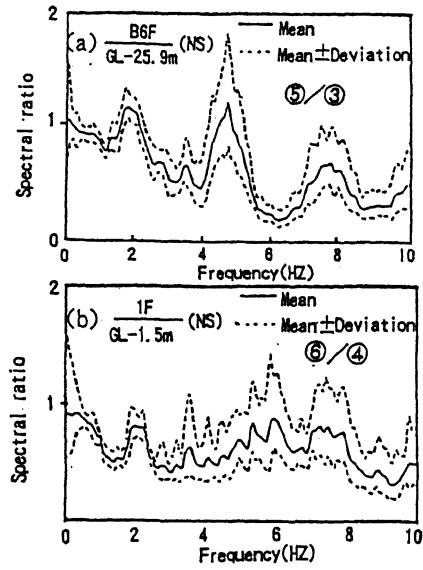


Fig.7 Averaged spectral ratio obtained from observed records in the building and the surrounding soil

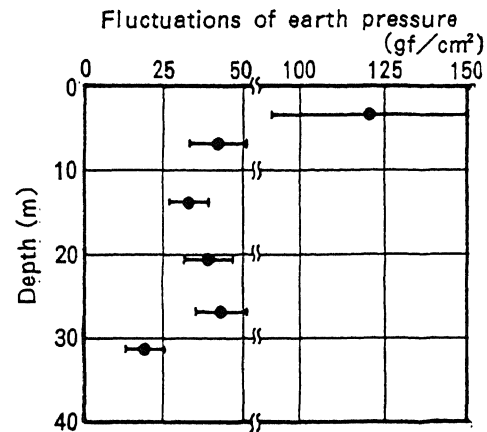


Fig.8 Maximum dynamic lateral pressure records distribution (Mean and Deviation)

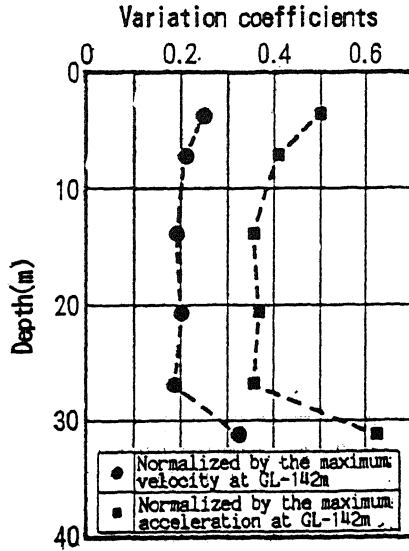


Fig.9 Distribution of variation coefficients

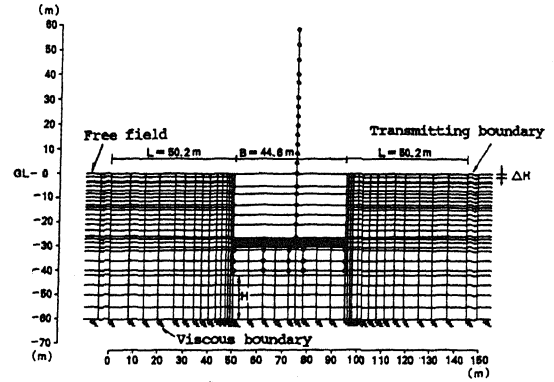


Fig.11 Finite Element Model for Analysis

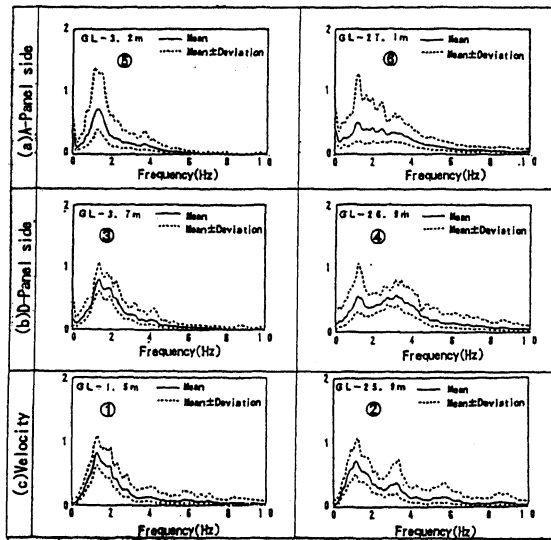


Fig.10 Comparison between normalized spectra obtained from dynamic lateral pressure records and that obtained from velocity records

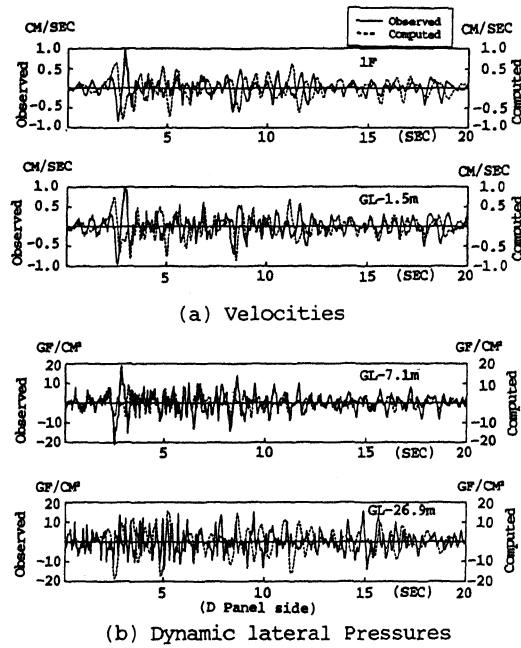
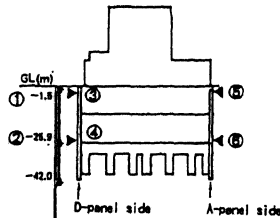
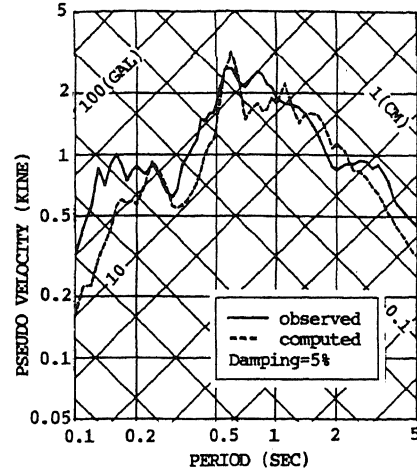
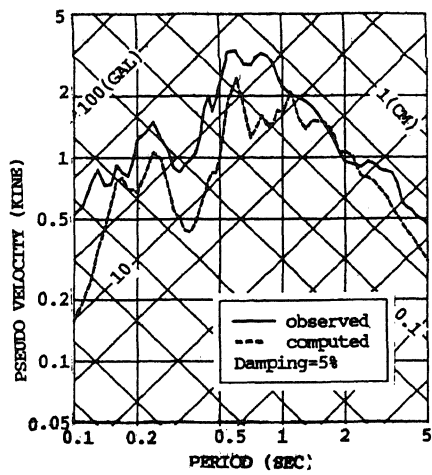


Fig.12 Comparison of Response Waveforms between Observed and Computed by FEM





(a) GL-1.5m(E-W Direction) (b) 1 F (E-W Direction)  
 Fig.13 Observed and Computed Response Spectra Based on the South-Western Ibaraki Pref. EQ  
 (M=5.6,Focal Depth=54km,Epicentral Distance=34km)

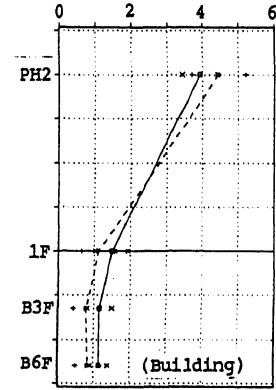
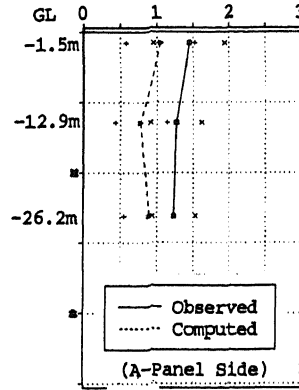
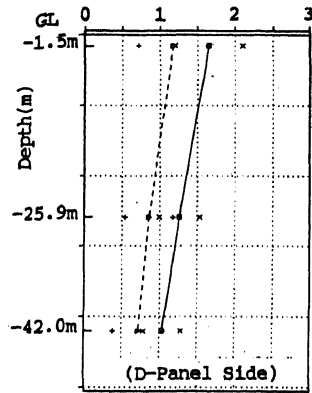


Fig.14 Distribution of maximum velocity compared with results computed by FEM  
 (Normalized by the Maximum Velocity at GL-142m, E-W direction) (Mean and Deviation)

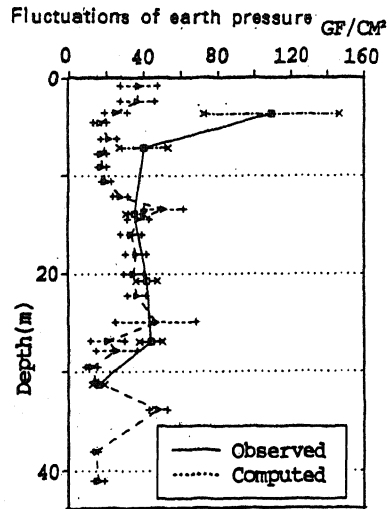


Fig.15 Distribution of maximum dynamic lateral pressure compared with results computed by FEM (Normalized by the Maximum Velocity at GL-142m) (Mean and Deviation)

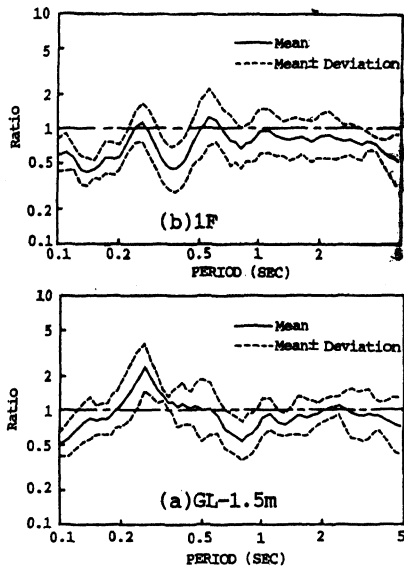


Fig.16 Averaged velocity response spectral ratio (Computed/Observed)